Check for updates

Received: 1 October 2020 | Revised: 8 March 2021 | Accepted: 14 March 2021

DOI: 10.1002/app.50768

ARTICLE

Applied Polymer SCIENCE WILEY

Tribo-material based on a UHMWPE/RGOC biocomposite for using in artificial joints

Ferda Mindivan[1] | **Alime Çolak**[2]

[1]Faculty of Engineering, Department of Bioengineering, Bilecik Seyh Edebali University, Bilecik, Turkey

[2]Biotechnology Application and Research Centre, Bilecik Seyh Edebali University, Bilecik, Turkey

Correspondence
Ferda Mindivan, Bilecik Seyh Edebali University, Faculty of Engineering, Department of Bioengineering, C Block, C240, Gülümbe Campus, 11230 Bilecik, Turkey.
Email: ferda.mindivan@bilecik.edu.tr and ferdagtekin@hotmail.com

Funding information
Bilecik Seyh Edebali University, Grant/Award Number: 2019-02.BŞEÜ.03-02

Abstract

Reduced graphene oxide (RGOC) filler that was green synthesized by vitamin C had been included in the ultrahigh molecular weight polyethylene (UHMWPE) matrix to produce biocomposite possessing improved properties especially against wear. The biocomposites filled with different loading (0.1, 0.3, 1.0, and 2.0 wt%) of RGOC was produced by a method of liquid phase ultrasonic mixing and then hot press molding. The structural analysis results of biocomposites showed that RGOC well-dispersed in polymer matrix and confirmed that there was interaction between the RGOC-UHMWPE. The biocomposite containing 2.0 wt% RGOC (UHMWPE/RGOC-2) gave the maximum microhardness and the value increased by 22. 5% compared with unfilled polymer. At the same RGOC content, the biocomposite had the highest thermal stability with residue content at 2.42%. The wear and friction behavior of biocomposites were carried out in a reciprocating friction testing machine under distilled water lubricating conditions. The UHMWPE/RGOC-2 biocomposite had the lowest friction coefficient value (0.034) and the wear rate of the biocomposite decreased by 44%, compared with that of unfilled UHMWPE. Furthermore, fatigue wear tracks were significantly reduced. This study suggests the use of this composite that had excellent tribological behavior as biomaterial instead of UHMWPE.

KEYWORDS

biomaterials, graphene and fullerenes, mechanical properties, nanotubes, structure-property relationships, thermogravimetric analysis

1 | INTRODUCTION

Polymeric biomaterials are more advantageous than metal and ceramic biomaterials due to their easy shaping, affordable cost, and the ability to provide the desired physical and chemical properties. Ultrahigh molecular weight polyethylene (UHMWPE) is known an acetabular component, which is self-lubricating, high-impact strength, low-friction coefficient, and chemical inertness.[1,2] However, wear problems of UHMWPE components are known to be a great disadvantage limiting the service life of implants.[1,3] Therefore, the most preferred method for improving the wear resistance and reducing the plastic deformation of UHMWPE is to increase the crosslink density within the amorphous phase of the polymer by gamma irradiation[3,4] but, this method is associated with an increased risk of oxidation and therefore the mechanical properties of the materials were negatively affected.[4] There has been the addition of vitamin E (α -tocopherol) in the UHMWPE matrix to prevent oxidation and to improve the mechanical properties of UHMWPE material. Vitamin E provides oxidation resistance by reacting with free radicals in

 © 2021 Wiley Periodicals LLC.

UHMWPE. However, vitamin E had a limited effect on the mechanical and thermal properties of UHMWPE.[3] Another common strategy to improve the mechanical, tribological, and biocompatibility properties is the addition of fillers.[5] For this purpose, inorganic fillers were used such as kaolin,[6] zirconium,[7] nano zinc oxide.[8] Various carbon materials such as carbon fiber, carbon black and carbon nanotubes have been used as fillers in UHMWPE matrix. However, due to the high cost and unsatisfactory performance of inorganic and organics filled UHMWPE composites, its use as implant material has been limited. These conditions significantly lead the production of low-cost and high-performance UHMWPE composites as implants.[1] Since graphene's successful isolation from graphite in 2004, too much effort has been made to obtain large quantities of this special material.[9,10] The remarkable performance of graphene and its derivatives are being studied in a wide spectrum of applications.[9] Along with its derivatives, particularly graphene oxide (GO) and reduced graphene oxide (RGO), GO is the product of oxidation reaction of graphite. Thus GO has rich oxygen containing functional groups such as hydroxyl, epoxide, carboxylic, ketone, and aldehyde groups on its basal and layer edge. The oxidation reaction affects properties of GO such as the electronic, optical and adsorption properties because it causes some defects, impurities, structural disorder, wrinkle, crack, fragmentation and other structural attributes. Thus, GO is converted through chemical or physical reduction reactions to other graphene derivative and it is named as RGO.[9,11] The properties of RGO are very same to the pristine graphene compare with GO because oxygenous functional groups of GO are eliminated through reduction process.[11] Even though a large amount of literature about the effect of GO[1,12–14] and graphene nanoplates (GNP),[5–13] on the mechanical and tribological performances of UHMWPE composites have been published, a very limited investigation has been carried out on the effect of RGO on UHMWPE. Bhattacharyya et al.[15] reported that UHMWPE nanocomposite films was produced with RGO but it was synthesized using phenyl hydrazine as reduction agent. But in this study, RGO was synthesized by green synthesis with vitamin C and coded as RGOC. Hydrazine derivatives are strong and most commonly used reducing agents but highly toxic and instability. These limit its large-scale application. Therefore, greener materials (amino acid, plant extracts, microorganisms, proteins, hormones etc.) were used to substitute toxic hydrazine used in GO reduction and their yields, performances were compared with hydrazine.[11] In this study, we think that green synthesis is more suitable for biomaterial applications. In the current study, the structural, thermal, mechanical, and tribological properties of UHMWPE/RGOC biocomposites with different RGOC contents were investigated.

2 | MATERIAL AND METHODS

GO was prepared from natural graphite (powder ~45 μm, Aldrich) by the modified Hummers method[16,17] and GO reduced with vitamin C to RGOC according to literature.[18] The detailed information about the production process of UHMWPE/RGOC biocomposites were described in previous literature.[19] A series of the biocomposites were prepared with the mass ratios (RGOC:UHMWPE) of 0.1, 0.3, 1.0, and 2.0 weight % (wt%). The codes of unfilled UHMWPE and these four biocomposites were UHMWPE, UHMWPE/RGOC-0.1, UHMWPE/RGOC-0.3, UHMWPE/RGOC-1, and UHMWPE/RGOC-2. Before characterization, the surfaces of the unfilled polymer and their biocomposites were ground using 400, 600, 800, 1000, and 1200 grit SiC paper and mechanically polished with a fine grade Al_2O_3 paste to achieve a certain surface uniformity. Finally, the surfaces were thoroughly degreased with distilled water and alcohol cleaned. The images of the prepared samples for characterization was given in Figure 1.

3 | CHARACTERIZATION

X-ray diffraction (XRD) data were collected at room temperature using a diffractometer (PAN analytical, Empyrean) between 5 and 35°of 2θ°. The scanning rate of the instrument was 2°/min. The crystallite size of the biocomposites was calculated by the following Scherrer Equation (1)[20] and the lattice strain, ε, was calculated based by the following Equation (2)[21]:

$$L = \frac{k.\lambda}{\beta.\cos\theta}, \quad (1)$$

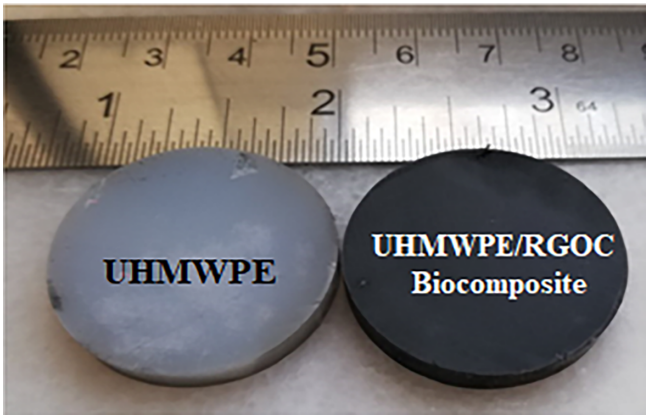

FIGURE 1 The images of unfilled UHMWPE and UHMWPE/RGOC biocomposite. RGOC, reduced graphene oxide; UHMWPE, ultrahigh molecular weight polyethylene [Color figure can be viewed at wileyonlinelibrary.com]

10974628, 2021, 31, Downloaded from https://onlinelibrary.wiley.com/doi/10.1002/app.50768 by Bilecik Seyh Edebali, Wiley Online Library on [22/12/2025]. See the Terms and Conditions (https://onlinelibrary.wiley.com/terms-and-conditions) on Wiley Online Library for rules of use; OA articles are governed by the applicable Creative Commons License

$$\varepsilon = \frac{\beta}{4.\tan\theta}, \quad (2)$$

where L is the crystallite size, K is a constant related to crystallite shape, β is the full width at half maximum (FWHM), λ is the wave length and θ is the peak position.

Fourier transform infrared spectroscopy (FTIR) spectra were recorded on a FTIR spectrophotometer (Spectrum 100, Perkin Elmer) in the wave number range of 4000–400 cm^{-1}. Field emission scanning electron microscopy (FE-SEM) was performed using a Supra 40VP, Zeiss scanning electron microscope with together energy-dispersive X-ray spectrometry (EDS) were used. The investigation of distribution of RGOC into UHMWPE matrix was done by high-resolution transmission electron microscopy (HR-TEM, JEOL 2100). Shimadzu microhardness tester was used to measure the hardness of the biocomposites prepared. Microhardness measurements of the studied biocomposites were measured using Vickers method with a load of 25 g where the reported values were in the average of 10 measurements. A reciprocating tribometer was used for all friction and wear tests. The wear tests on all biocomposites were performed under a constant load of 5 N at a sliding velocity of 1.7 cm s^{-1}, while sliding distance was 50 m. The counter body was an Al_2O_3 ball with 10 mm diameter. The wear rate was calculated by analyzing width and depth of wear scars with the help of a contact stylus profilometer (SJ400). The Al_2O_3 counterface surfaces and the surfaces of biocomposites that treated by acid etching were examined under an optical microscope (OM). At least three successive wear tests were performed for each biocomposite and the reported values (wear rates and friction coefficient values) were in the average of three measurements. In order to examine the thermal stability of the biocomposites, Thermogravimetric (TG) analysis (TGA, STA 409, Netzsch) was conducted at a heating rate of 20°C/min from ambient temperature to 600°C under a nitrogen atmosphere. Differential scanning calorimetry (DSC, STA 409, Netzsch) analysis was performed by heating the samples from 20 C to 600 C in nitrogen atmosphere at a heating rate of 20 C/min. The crystallinity (X_c) of UHMWPE and biocomposites obtained by DSC was calculated according to the following equations Equation (3)[3,4,13] and Equation (4),[22] respectively:

$$X_c\,(\%) = \frac{\Delta H_c}{\Delta H_f} * 100. \quad (3)$$

$$X_c\,(\%) = \frac{\Delta H_c}{\Delta H_f (1 - w_f)} * 100. \quad (4)$$

ΔH_c is the heat fusion of the UHMWPE and biocomposites obtained from DSC analysis, ΔH_f is the fusion enthalpy of 100% crystalline UHMWPE (ΔH_f = 289 $J/g\ f$)[3,4] and W_f is the mass fraction.

4 | RESULTS AND DISCUSSION

4.1 | XRD and DSC analysis

The crystalline structures of unfilled UHMWPE together with their biocomposites were investigated by the XRD and DSC analysis. Figure 2 showed XRD patterns of unfilled UHMWPE and all biocomposites. The XRD pattern of unfilled UHMWPE exhibited the sharp characteristic peaks in two theta regions at 2θ° = 21.5° (110) and 2θ° = 23.8° (200), which corresponds to the orthorhombic phase of semi crystalline UHMWPE matrix.[23] The biocomposites prepared by a filling of RGOC into UHMWPE exhibited two peaks of similar diffraction peaks to that of the matrix, and the intensity of diffraction peaks presented a decreasing at all filler contents. And also, no graphene diffraction peak was observed for all biocomposites due to uniform dispersion in the polymer matrix, except the crystalline diffraction peaks of the UHMWPE matrix.[24] Ahmet et al.[25] prepared ultrahigh-molecular-weight polyethylene/high-density polyethylene (UHMWPE/HDPE) blends using hydroxyapatite (HA) as the reinforcing filler. The intensity of both XRD diffraction peaks of PE and composites reduced which was attributed to modification of the mechanical and thermal properties of the prepared samples. It was found that, any diffraction peaks were not observed except crystalline peaks of the UHMWPE, GO layers were homogeneously dispersed into the UHMWPE matrix. Also, Pang with co-workers[26] experimentally examined the effects of

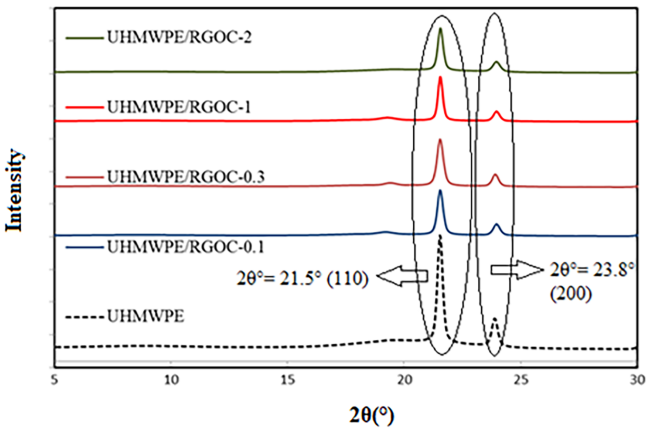

FIGURE 2 XRD patterns of unfilled UHMWPE and UHMWPE/RGOC biocomposites. RGOC, reduced graphene oxide; UHMWPE, ultrahigh molecular weight polyethylene; XRD, X-ray diffraction [Color figure can be viewed at wileyonlinelibrary.com]

10974628, 2021, 31, Downloaded from https://onlinelibrary.wiley.com/doi/10.1002/app.50768 by Bilecik Seyh Edebali, Wiley Online Library on [22/12/2025]. See the Terms and Conditions (https://onlinelibrary.wiley.com/terms-and-conditions) on Wiley Online Library for rules of use; OA articles are governed by the applicable Creative Commons License

GO content on mechanical and thermal properties of GO/UHMWPE composites. The characteristic peaks of GO were not appeared at XRD analysis results and the result demonstrated that GO was fully exfoliated within composites. As a result, in this study, the addition of RGOC filler changed the crystal structure of the polymer and the absence of an additional peak in the XRD diffractogram indicated that the filler was homogeneously distributed in the matrix.

The values of 2θ°, d-spacing, crystalline size, and micro strain of biocomposites with different content of RGOC were shown in Table 1. 2θ° and d-spacing values of all biocomposites had the same results with each other. In 0.1 and 0.3 wt% RGOC, the crystalline size of (110) plane decreased; when the loading content was 1.0 wt% RGOC, the increase in the crystallite size achieving 12%, for comparison with unfilled UHMWPE. And also, the UHMWPE/RGOC-2 biocomposite reached to the crystalline size value of the unfilled polymer. The crystalline size value of (200) plane decreased in all biocomposites compared with the unfilled polymer. Uflyand et al.[27] reported that the influence of fillers on the crystallization process of polymer materials were depend on some factors, for example, the size of the filler particles, their potent surface, the crystalline size of the unfilled polymer and the degree of interaction between the unfilled polymer and the fillers. Fillers can reduce crystallinity due to bind polymer chains or increase crystalline size as nucleation centers in the polymer matrix. UHMWPE/RGOC-1 biocomposite acted as nucleating agents which help increasing crystalline size of UHMWPE in (110) plane, but in low amount of filler, RGOC caused to bind polymer chains and reduced crystalline size. In the addition of 2.0 wt% RGOC, the same crystalline size appeared with the unfilled polymer and the addition of 1.0 wt% RGOC was the maximum addition amount that increased the crystalline size of the structure. The reduction of the crystalline sizes of (200) plane was associated that all the added wt% content of RGOC did not act as a nucleation center in the UHMWPE matrix. We thought that all wt% contents of RGOC binded polymer chains. As seen in Table 1, the micro strain values of the (110) plane increased at the addition of 0.1 and 0.3 wt% RGOC, while it remained same as the UHMWPE at the addition of 1.0 wt% and 2.0 wt% RGOC. In the (200) plane, the micro strain values in all biocomposites increased compared to the unfilled polymer. The addition of low wt% RGOC in (110) plane increased micro strain values due to chain binding during the crystallization process. The addition of low wt% RGOC in (110) plane increased micro strain values due to chain binding during the crystallization process. There was no significant change in micro strain values but crystalline size increased in addition of 1.0 wt % RGOC compared to the unfilled UHMWPE because this amount of RGOC did not disturb the chain linearity and made to stack easier. For the (200) plane, the decrease in crystalline size of all biocomposites caused an increase in micro strain values. In addition to XRD analysis, the crystallinity of synthesized biocomposites were investigated by DSC analysis. Figure 3 showed the DSC thermograms and the melting temperatures, the degree of crystallinity and the heat of fusion (ΔH_f) values of unfilled polymer and biocomposites were summarized in Table 2. Unfilled UHMWPE and all biocomposites exhibited crystal peaks with melting points. The melting temperatures remained constant at RGOC contents of 0.1 and 0.3 wt% but the heat of fusion (ΔH_f) values of these biocomposites was not calculated by calorimetry. However, increases in RGOC content caused rises in the melting temperatures. As shown in Table 2, in comparison to the unfilled polymer with melting temperatures of 145.54 C, the UHMWPE/RGOC-1 biocomposite showed

TABLE 1 D-spacing, crystallite size, and micro-strain of unfilled UHMWPE and UHMWPE/RGOC biocomposites

Sample	2θ (°)	D-Spacing (A°)	Crystallite Size (A°)	Micro-strain (%)
UHMWPE	21.525	4.128	368.124	0.561
	23.870	3.727	334.017	0.558
UHMWPE/RGOC-0.1	21.531	4.127	332.715	0.620
	23.946	3.216	280.492	0.662
UHMWPE/RGOC-0.3	21.527	4.127	303.651	0.679
	23.892	3.724	304.862	0.610
UHMWPE/RGOC-1	21.535	4.126	412.317	0.500
	23.945	3.716	304.891	0.610
UHMWPE/RGOC-2	21.54	4.125	368.134	0.560
	23.941	3.717	259.764	0.715

Abbreviations: RGOC, reduced graphene oxide; UHMWPE, ultrahigh molecular weight polyethylene.

10974628, 2021, 31, Downloaded from https://onlinelibrary.wiley.com/doi/10.1002/app.50768 by Bilecik Seyh Edebali, Wiley Online Library on [22/12/2025]. See the Terms and Conditions (https://onlinelibrary.wiley.com/terms-and-conditions) on Wiley Online Library for rules of use; OA articles are governed by the applicable Creative Commons License

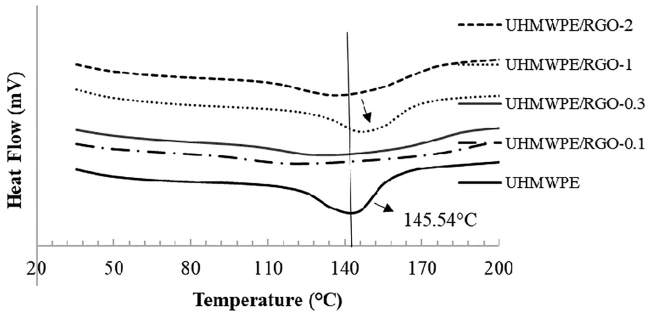

FIGURE 3 DSC thermograms of unfilled UHMWPE and UHMWPE/RGOC biocomposites. DSC, differential scanning calorimetry; RGOC, reduced graphene oxide; UHMWPE, ultrahigh molecular weight polyethylene

TABLE 2 DSC characteristics of unfilled UHMWPE and UHMWPE/RGOC biocomposites

	Tm (°C)	ΔH_c (J/g)	% Crystallinity
UHMWPE	145.54	100.34	34.72
UHMWPE/RGOC-0.1	145.51	–	–
UHMWPE/RGOC-0.3	145.74	–	–
UHMWPE/RGOC-1	155.51	112.33	39.26
UHMWPE/RGOC-2	147.14	101.87	35.97

Abbreviations: RGOC, reduced graphene oxide; UHMWPE, ultrahigh molecular weight polyethylene.

the highest melting temperature value (155.51 C). The melting temperature increased to 147.14 C with the 2.0 wt% RGOC addition, but it was still higher than that of unfilled UHMWPE. Thus, it was reasonable to attribute the significant improvement of thermal stability for UHMWPE/RGOC-1 and UHMWPE/RGOC-2 biocomposites to the good interactions between filler-polymer interface. Similarly, the degree of crystallinity increased at same biocomposites and the DSC results were consistent with the results obtained from XRD studies. As a result, the addition of 1.0 wt% RGOC was the maximum addition amount that increased the crystallinity of the structure.

4.2 | FTIR analysis

FTIR spectrum of the unfilled UHMWPE and all biocomposites over wavenumbers from 4000 to 400 cm^{-1} were shown in Figure 4 and the band assignments of all biocomposites were recorded in the transmittance mode and they were listed in Table 3. The characteristic bands of unfilled UHMWPE at 2915.92–2848.69 cm^{-1} could be assigned to C—H stretching vibrations. The bands at 1463.04 and 1261.25 cm^{-1} were designated to CH_2 bending and twisting vibrations, respectively.[28–30] The band at 718.47 cm^{-1} could be attributed to the CH_2 rocking vibration (Table 3); indicating the long molecular chain and high-degree polymerization of UHMWPE.[26] With the dispersion of RGOC in UHMWPE/RGOC biocomposites containing 0.1, 1.0, and 2.0 wt% RGOC, the peaks at 2962.84–2848.69 cm^{-1} (C—H stretching), 1463.04 cm^{-1} (CH_2 bending) and 718.47 cm^{-1} (CH_2 rocking) sharpened, suggesting that RGOC has interacted with the molecular structure of unfilled UHMWPE.[31] As seen from Figure 4, it was seen that the intensity of all vibration peaks (C—H stretching, CH_2 bending and CH_2 rocking) of the UHMWPE/RGOC-0.3 biocomposite decreased compared to both unfilled UHMWPE and other biocomposites. This observed change might be due to the occurrence of disruption of existing bonds and the formation of new bonds, and the mobility of polymer chains due to interactions between matrix-filler.[32] Furthermore, the peak of CH_2 twisting and —(C—O—C) vibrations at 1261.25 and 1053.24 cm^{-1} in unfilled UHMWPE, respectively, as seen in Figure 4 and Table 3, they lost completely in the FTIR spectra of UHMWPE/RGOC-0.1 biocomposite, but the intensity of same peak decreased at the addition of 0.3, 1.0 and 2.0 wt% RGOC. This result showed that the addition of RGOC to the UHMWPE matrix appeared to significantly affect the twisting vibration of the CH_2 and —(C—O—C) carbon bonds vibration. Also, the interaction of the filler-matrix was supported by XRD analysis results.

4.3 | FE-SEM, OM, HR-TEM, and EDS analysis

Figure 5 showed the FE-SEM images of the surfaces of unfilled UHMWPE and all biocomposites at the same magnification and EDS elemental maps of carbon and oxygen. And also, the surfaces of unfilled UHMWPE and all biocomposites were treated by acid etching (7% potassium permanganate/concentrated sulfuric acid) in order to expose the crystalline structures and the crystalline structures were observed by OM at Figure 6. As shown in Figure 5, the surface of the unfilled UHMWPE was relatively flat, but there were also wrinkled areas. The treated image of unfilled UHMWPE was observed similarly with the literature and attributed its low degree of crystallinity and loose crystal structure (Figure 5).[14] This structure was demonstrated with dark traces in treated surface image of unfilled UHMWPE at Figure 6. This dark traces showed crystal regions of structure. Park et al.[33] reported similar image for dispersion of the pre-treated filler material in the a polymer matrix by using OM. The surface

10974628, 2021, 31, Downloaded from https://onlinelibrary.wiley.com/doi/10.1002/app.50768 by Bilecik Seyh Edebali, Wiley Online Library on [22/12/2025]. See the Terms and Conditions (https://onlinelibrary.wiley.com/terms-and-conditions) on Wiley Online Library for rules of use; OA articles are governed by the applicable Creative Commons License

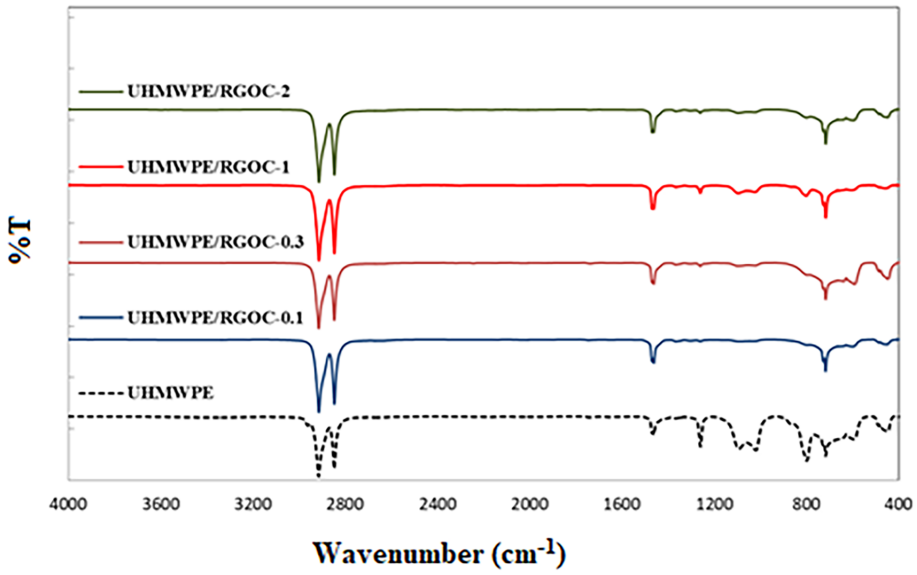

FIGURE 4 FTIR spectrum of unfilled UHMWPE and UHMWPE/RGOC biocomposites. FTIR, Fourier transform infrared spectroscopy; RGOC, reduced graphene oxide; UHMWPE, ultrahigh molecular weight polyethylene [Color figure can be viewed at wileyonlinelibrary.com]

TABLE 3 Functional groups and wavenumbers obtained from FTIR spectrum of unfilled UHMWPE and UHMWPE/RGOC biocomposites

Sample	UHMWPE	UHMWPE/RGOC-0.1	UHMWPE/RGOC-0.3	UHMWPE/RGOC-1	UHMWPE/RGOC-2
Functional group	Wavenumber (cm^{-1})				
—CH_2 asymmetric stretching vibrations	2915.92	2915.37	2915.94	2914.97	2914.94
—CH_2 symmetric stretching vibrations	2848.69	2848.17	2848.55	2848.05	2848.08
—CH_2 bending vibrations	1463.04	1462.79	1463.03	1463.19	1463.16
—CH_2 twisting vibration	1261.25	–	1261.68	1261.99	1261.87
—(C—O—C) vibration	1053.24	–	1052.87	1053.54	1053.68
—CH_2 rocking vibration	718.47	718.86	718.49	718.34	718.16

Abbreviations: RGOC, reduced graphene oxide; UHMWPE, ultrahigh molecular weight polyethylene.

morphology and treated image of the UHMWPE/RGOC-1 biocomposite exhibited an irregular structure with heterogeneous nucleation zones (Figure 5). It was understood that the crystallinity of the UHMWPE/RGOC-1 biocomposite increased due to the large surface area of the graphene and this result was supported by DSC analysis (Table 2). And also, treated surface image of UHMWPE/RGOC-1 biocomposite was presented much more dark traces than other biocomposites at Figure 6. This image was attributed its dense crystal structure. The FE-SEM surface images of UHMWPE/RGOC-0.1 and UHMWPE/RGOC-0.3 biocomposites showed irregular structure in some areas but they had flatter morphology generally than the surface image of the UHMWPE/RGOC-1 biocomposite. OM images of the same biocomposites in Figure 6 showed rare and little traces. The FE-SEM surface image of the UHMWPE/RGOC-2 biocomposite was irregular compared to the surface images of UHMWPE/RGOC-0.1 and UHMWPE/RGOC-0.3 biocomposites, but UHMWPE/RGOC-2 had more uniform morphology than the surface of the UHMWPE/RGOC-1 biocomposite. Treated surface image of UHMWPE/RGOC-2 biocomposite had few, but much more broad dark traces than other biocomposites and unfilled UHMWPE. All FE-SEM and OM images revealed that the addition of 1.0 wt% RGOC to the polymer matrix was the maximum filler amount that increased the crystallinity of the structure. The addition of 0.1% and 0.3 wt % RGOC reduced crystallinity by wrapping polymer chains but the addition of 1.0 wt% RGOC increased the crystallinity by nucleation effect and 2.0 wt% content was no serious effect on crystallinity. This result was supported by XRD and DSC analysis. According to the XRD and DSC analysis results (Tables 1 and 2), the

10974628, 2021, 31, Downloaded from https://onlinelibrary.wiley.com/doi/10.1002/app.50768 by Bilecik Seyh Edebali, Wiley Online Library on [22/12/2025]. See the Terms and Conditions (https://onlinelibrary.wiley.com/terms-and-conditions) on Wiley Online Library for rules of use; OA articles are governed by the applicable Creative Commons License

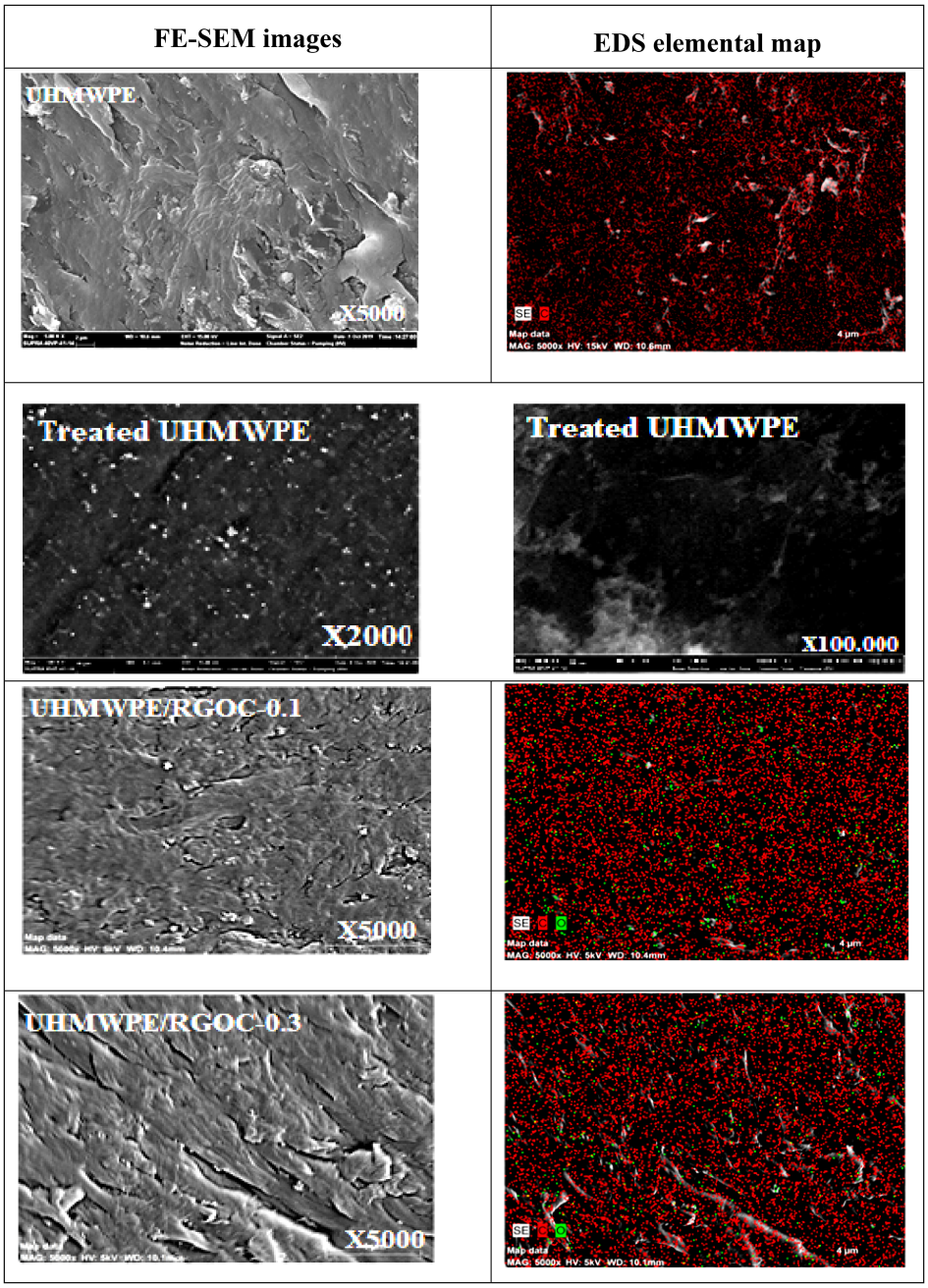

FIGURE 5 FE-SEM images of unfilled UHMWPE and UHMWPE/RGOC biocomposites (magnification 5 000 kx) and EDS elemental map of carbon and oxygen. FE-SEM, Field emission scanning electron microscopy; RGOC, reduced graphene oxide; UHMWPE, ultrahigh molecular weight polyethylene [Color figure can be viewed at wileyonlinelibrary.com]

UHMWPE/RGOC-1 biocomposite had the highest crystallite size (412.317 A°) and % crystallinity value (38.87). The UHMWPE/RGOC-0.1 and UHMWPE/RGOC-0.3 biocomposites had the lowest crystallite sizes (332.715 A° and 303.651 A°, respectively) and also the UHMWPE/RGOC-2 biocomposite had the similar crystallite size (368.134 A°) as the unfilled UHMWPE (368.124 A°) but % crystallinity value of the same biocomposite (35.25) was higher than unfilled polymer (Table 2). Broad dark traces supported this % crystallinity result at OM image of UHMWPE/RGOC-2 biocomposite (Figure 6). The EDS elemental mapping results of all biocomposites confirmed that oxygen groups of RGOC were uniformly distributed in the UHMWPE matrix. Green dots represented the oxygen elements in the EDS maps. The dispersion of oxygen was very important because only RGOC had oxygen containing

10974628, 2021, 31, Downloaded from https://onlinelibrary.wiley.com/doi/10.1002/app.50768 by Bilecik Seyh Edebali, Wiley Online Library on [22/12/2025]. See the Terms and Conditions (https://onlinelibrary.wiley.com/terms-and-conditions) on Wiley Online Library for rules of use; OA articles are governed by the applicable Creative Commons License

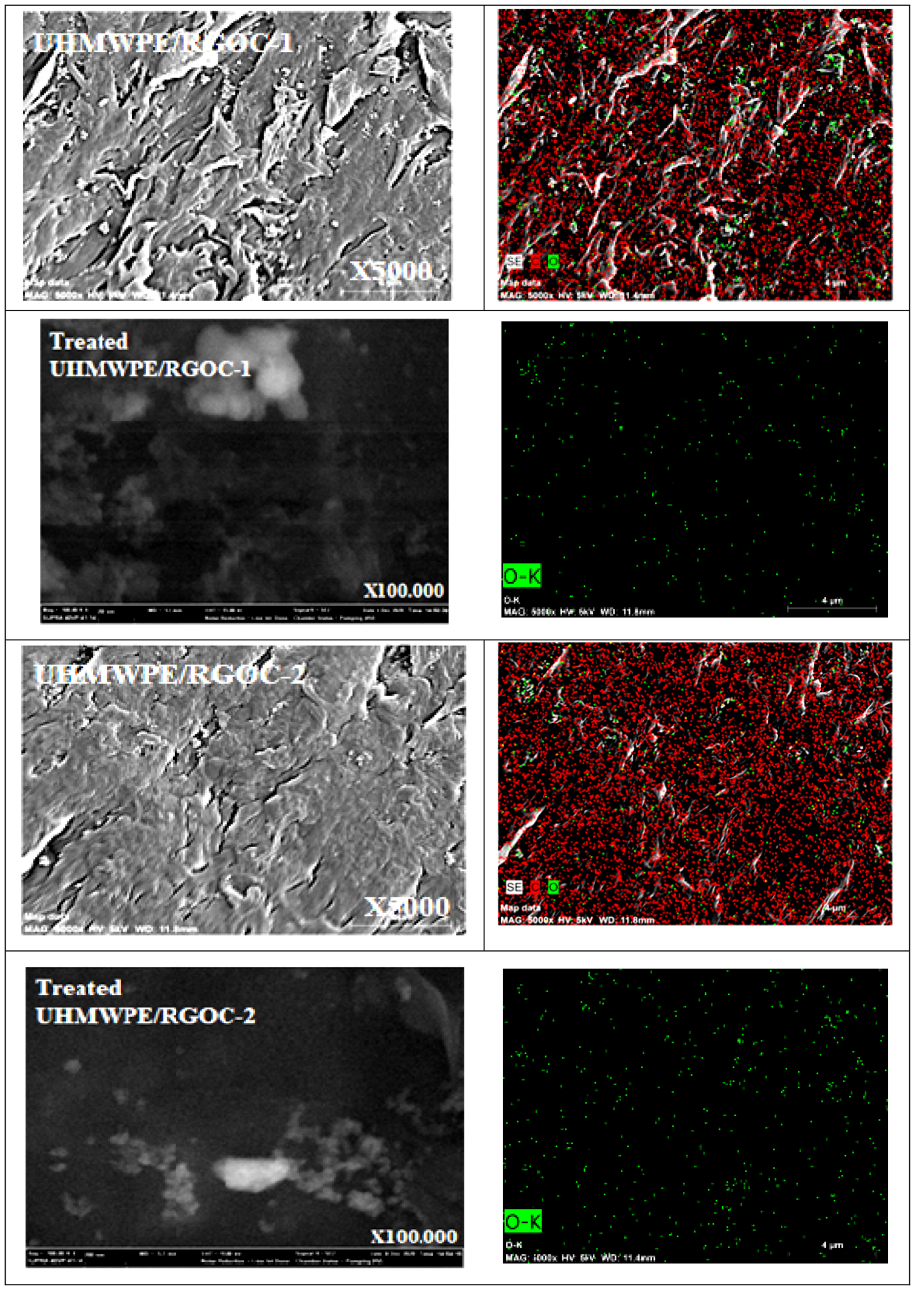

FIGURE 5 (Continued)

functional groups in the matrix.[19] The results obtained from the EDS analysis were compatible with XRD results. The characteristic peak of graphene was not seen at the XRD diffractogram of all biocomposites (Figure 2) which proved that the graphene was homogeneously distributed in the polymer matrix. And also, Figure 7 showed the uniform distribution of RGOC in the UHMWPE matrix with HR-TEM images of the prepared UHMWPE/RGOC-1 and UHMWPE/RGOC-2 biocomposites. Similar sized HR-TEM images were reported in the literature to show the homogeneous distribution of other graphene derivatives.[34,35]

4.4 | Microhardness analysis

Figure 8 showed the microhardness results for unfilled UHMWPE and all biocomposites. The microhardness values showed an increase with the increase in RGOC content. The UHMWPE/RGOC-2 biocomposite gave the maximum microhardness value (7.17 MPa) which was an increment of 22.5%, compared with unfilled polymer (5.86 MPa) as shown in Figure 6. As discussed in the FE-SEM and HR-TEM analysis section, the hardness, that is, the resistance to indentation increased because of the

10974628, 2021, 31, Downloaded from https://onlinelibrary.wiley.com/doi/10.1002/app.50768 by Bilecik Seyh Edebali, Wiley Online Library on [22/12/2025]. See the Terms and Conditions (https://onlinelibrary.wiley.com/terms-and-conditions) on Wiley Online Library for rules of use; OA articles are governed by the applicable Creative Commons License

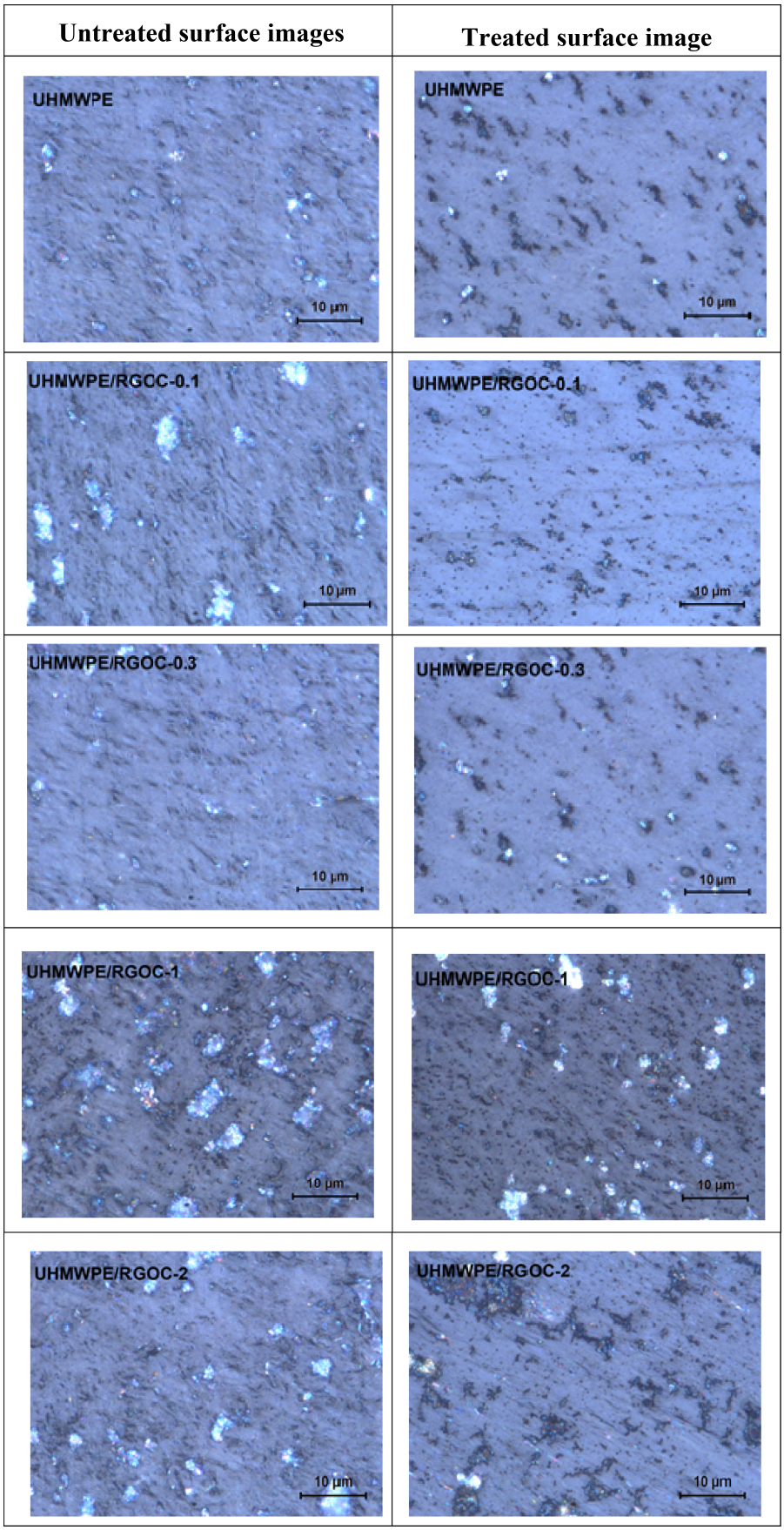

FIGURE 6 OM images of the surface crystal structures of unfilled UHMWPE and biocomposites. UHMWPE, ultrahigh molecular weight polyethylene [Color figure can be viewed at wileyonlinelibrary.com]

10974628, 2021, 31, Downloaded from https://onlinelibrary.wiley.com/doi/10.1002/app.50768 by Bilecik Seyh Edebali, Wiley Online Library on [22/12/2025]. See the Terms and Conditions (https://onlinelibrary.wiley.com/terms-and-conditions) on Wiley Online Library for rules of use; OA articles are governed by the applicable Creative Commons License

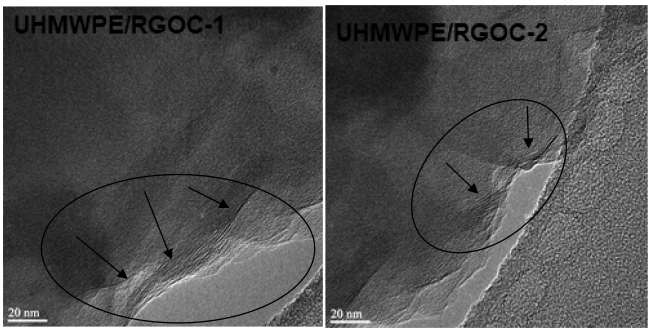

FIGURE 7 HR-TEM images of the UHMWPE/RGOC-1 and UHMWPE/RGOC-2 biocomposites. HR-TEM, high-resolution transmission electron microscopy; RGOC, reduced graphene oxide; UHMWPE, ultrahigh molecular weight polyethylene

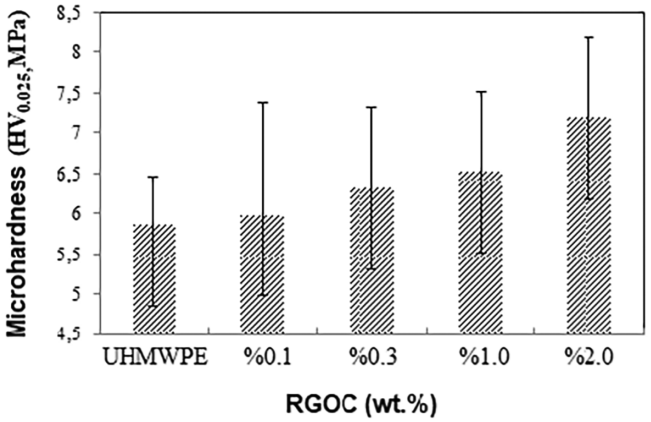

FIGURE 8 The microhardness results of the unfilled UHMWPE and UHMWPE/RGOC biocomposites. RGOC, reduced graphene oxide; UHMWPE, ultrahigh molecular weight polyethylene

homogeneous distribution of RGOC in the polymer matrix.[1] In other words, the two-dimensional structure of RGOC increased its capacity to carry and transfer loads. The addition of RGOC to the matrix also changed the crystallinity of the structure. In UHMWPE, rigidity and hardness depend on crystallinity. It is widely reported in the literature that the increase in mechanical properties are proportional to the increase in crystallinity.[14]

4.5 | Wear analysis

The friction coefficients and wear rates of the unfilled UHMWPE and all biocomposites were shown in Table 4 and Figure 9, respectively. As can be confirmed from Table 4, the all biocomposites exhibited a continuously decreasing trend with the increasing of RGOC addition. The low-friction coefficient of about 0.034 was obtained for water sliding condition for UHMWPE/RGOC-2

TABLE 4 The friction coefficient values of unfilled UHMWPE and UHMWPE/RGOC biocomposites

Sample	Friction coefficients
UHMWPE	0.089 ± 0.0021
UHMWPE/RGOC-0.1	0.074 ± 0.0045
UHMWPE/RGOC-0.3	0.068 ± 0.0053
UHMWPE/RGOC-1	0.054 ± 0.0018
UHMWPE/RGOC-2	0.034 ± 0.0011

Abbreviations: RGOC, reduced graphene oxide; UHMWPE, ultrahigh molecular weight polyethylene.

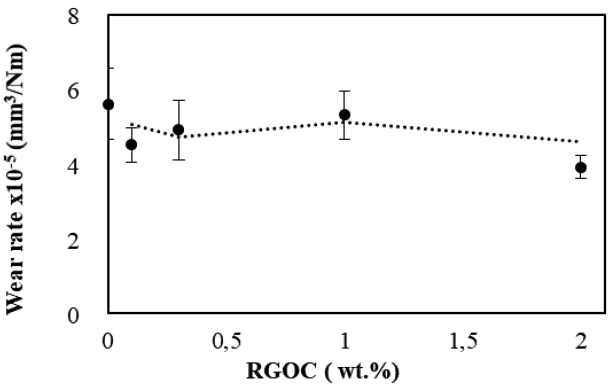

FIGURE 9 Wear rate of unfilled UHMWPE and UHMWPE/RGOC biocomposites. RGOC, reduced graphene oxide; UHMWPE, ultrahigh molecular weight polyethylene

biocomposite. This biocomposite with the highest content of RGOC had the lowest friction coefficient value. The lubricating effect of both distilled water and RGOC decreased friction coefficient. Graphene is considered to be an important solid lubricant in improving the tribological properties of polymer composites.[36] The wear rate of the UHMWPE/RGOC-2 biocomposite decreased by 44%, compared with that of unfilled UHMWPE. The improvement in load transfer is attributed to homogeneous dispersion of RGOC in the UHMWPE matrix.[14] Even though a large amount of literature about the effect of graphene derivatives on the wear performances of UHMWPE composites have been published, no investigation has been carried out on the effect of RGOC that synthesis with vitamin C on UHMWPE. Consequently, the vitamin C is a good candidate for replacement of harmful/toxic reducing agents in the synthesis of RGO instead of other graphene derivatives.

The FE-SEM images of wear tracks for the unfilled UHMWPE and all biocomposites shown in Figure 10. It could be seen that the worn surface of unfilled UHMWPE were thin grooves in the low-magnified image but the cracked surface layer of the polymer showed that the dominant mechanism was fatigue wear in the high-

10974628, 2021, 31, Downloaded from https://onlinelibrary.wiley.com/doi/10.1002/app.50768 by Bilecik Seyh Edebali, Wiley Online Library on [22/12/2025]. See the Terms and Conditions (https://onlinelibrary.wiley.com/terms-and-conditions) on Wiley Online Library for rules of use; OA articles are governed by the applicable Creative Commons License

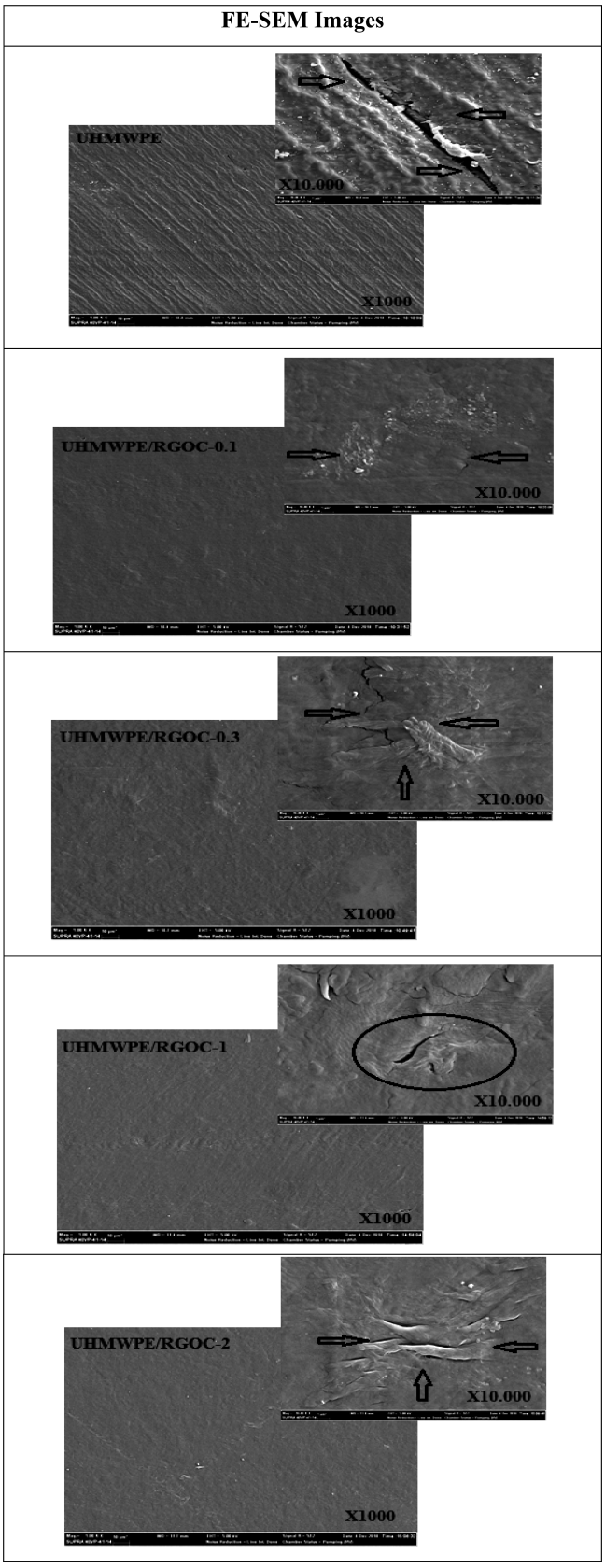

FIGURE 10 Low and high magnification FE-SEM micrographs of wear tracks generated on the unfilled UHMWPE and the UHMWPE/RGOC biocomposites. FE-SEM, Field emission scanning electron microscopy; RGOC, reduced graphene oxide; UHMWPE, ultrahigh molecular weight polyethylene

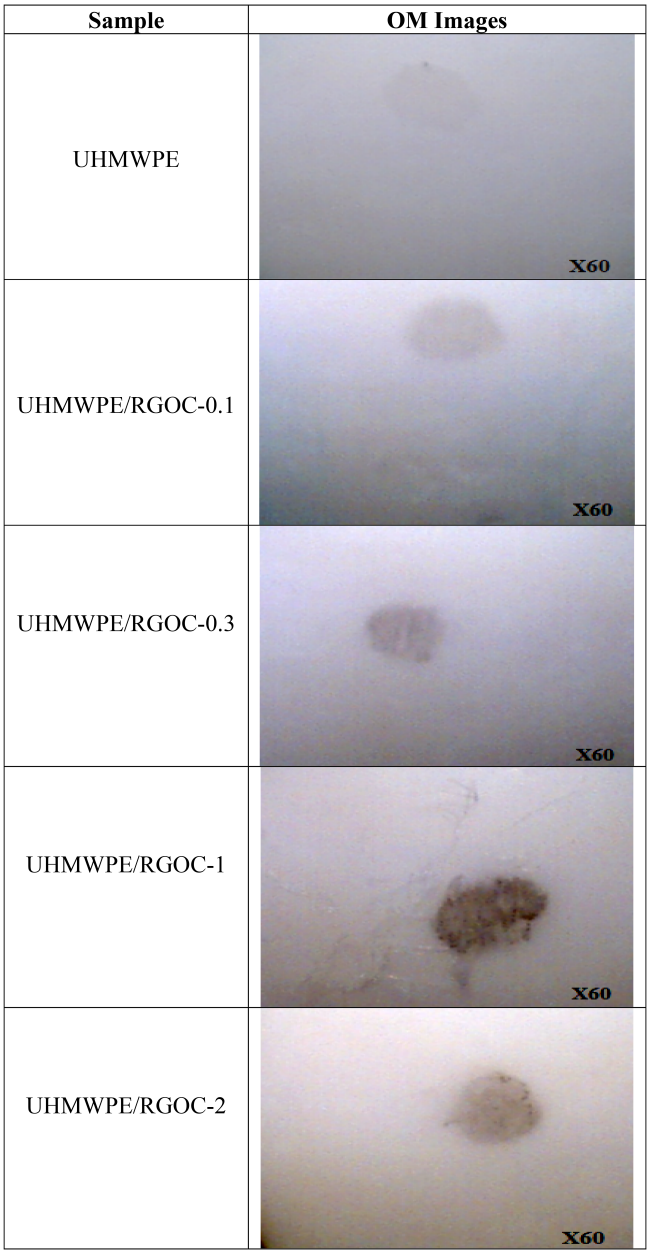

FIGURE 11 OM images of the Al_2O_3 balls sliding against the unfilled UHMWPE and the UHMWPE/RGOC biocomposites. RGOC, reduced graphene oxide; UHMWPE, ultrahigh molecular weight polyethylene [Color figure can be viewed at wileyonlinelibrary.com]

magnified image.[19] The low-magnified image of UHMWPE/RGOC-0.1 biocomposite showed relatively flat surface but fatigue wear tracks were seen in the high-magnified image. The worn surfaces of other biocomposites seemed generally straight in low-magnified images. In addition, from the high-magnified images shown in Figure 10, it was clear that they had adhesive wear tracks and significant fatigue tear. As a result, with increasing of RGOC filler amount, the worn surfaces of the biocomposites were flattened, and the grooves were disappeared on the surface of the unfilled polymer.

10974628, 2021, 31, Downloaded from https://onlinelibrary.wiley.com/doi/10.1002/app.50768 by Bilecik Seyh Edebali, Wiley Online Library on [22/12/2025]. See the Terms and Conditions (https://onlinelibrary.wiley.com/terms-and-conditions) on Wiley Online Library for rules of use; OA articles are governed by the applicable Creative Commons License

Filler-matrix interaction was provided, and the wear resistance was increased significantly by graphene. OM analyses of the surface morphologies of Al_2O_3 counterface were evaluated in Figure 11. Unfilled UHMWPE and all biocomposites except the UHMWPE/RGOC-1 biocomposite had a thin and uniform transfer film on the Al_2O_3 ball but a patchy tribofilm produced from UHMWPE/RGOC-1 biocomposite was observed (Figure 10). Because this biocomposite had the highest wear rate than that of other biocomposites.

5 | CONCLUSIONS

RGOC filler prepared by green reduction with Vitamin C were added into the UHMWPE matrix, to improve thermal, mechanical, and tribological properties of biocomposites. Liquid phase ultrasonic mixing and then hot press molding was used to prepared biocomposites. The addition of RGOC changed the crystallinity of the structure. The interaction of the filler-matrix and homogeneous distribution of RGOC in polymer matrix was achieved. The addition of 2.0 wt% RGOC induced the best thermal stability and microhardness value compared to unfilled UHMWPE and other biocomposites. With the RGOC content increases, the frictional coefficient of the UHMWPE/RGOC biocomposites were decreased. UHMWPE/RGOC-2 biocomposite had the lowest friction coefficient value due to lubricating effect of both distilled water and RGOC. The wear rate of the same biocomposite decreased by 44%, compared with that of unfilled UHMWPE. With increasing of RGOC filler amount fatigue wear tracks on the worn surfaces of the biocomposites were decreased significantly. We think based on the green synthesis that RGOC is an excellent wear-resistant filler for UHMWPE and acetabular prosthesis components.

ACKNOWLEDGEMENT

The authors thank the financial support of the research foundation (Project no: 2019-02.BŞEÜ.03-02) of Bilecik Seyh Edebali University.

ORCID

Ferda Mindivan https://orcid.org/0000-0002-6046-2456
Alime Çolak https://orcid.org/0000-0002-1311-8644

REFERENCES

[1] Z. Tai, Y. Chen, Y. An, X. Yan, Q. Xue, *Tribol. Lett.* **2012**, *46*, 55.
[2] S. Firdous, M. Fuzail, M. Atif, M. Nawaz, *Optik.* **2009**, *122*, 99.
[3] L. Melk, N. Emami, *Compos. B Eng.* **2018**, *146*, 20.
[4] F. Alam, M. Choosri, T. K. Gupta, K. M. Varadarajan, D. Choi, S. Kumar, *Mater. Sci. Eng. B-Adv.* **2019**, *241*, 82.
[5] A. Chih, A. Ansón-Casaos, J. A. Puértolas, *Tribol. Int.* **2017**, *116*, 295.
[6] G. F. Gong, H. Y. Yang, X. Fu, *Wear* **2004**, *256*, 88.
[7] K. Plumlee, C. J. Schwartz, *Wear* **2009**, *267*, 710.
[8] A. J. K. Prasad, H. S. Yeshvantha, A. T. Chandrakant, G. J. Basvaraj. *Mater. Today: Proc.* **2018**, *5*, 2619.
[9] X. J. Lee, B. Y. Z. Hiew, K. C. Lai, L. Y. Lee, S. Gan, S. Thangalazhy-Gopakumara, S. Rigby. *J. Taiwan Inst. Chem. E.* **2019**, *98*, 163.
[10] C. Gómez-Navarro, J. C. Meyer, R. S. Sundaram, A. Chuvilin, S. Kurasch, M. Burghard, K. Kern, U. Kaiser, *Nano Lett.* **2010**, *10*, 1144.
[11] M. Tahriri, M. Del Monico, A. Moghanian, M. Tavakkoli Yaraki, R. Torres, A. Yadegari, L. Tayebi, *Mater. Sci. Eng. C.* **2019**, *102*, 171.
[12] H. S. Vadivel, A. Golchin, N. Emami, *Tribol Int.* **2018**, *124*, 169.
[13] A. Golchin, A. Wikner, N. Emami, *Tribol Int.* **2016**, *95*, 156.
[14] W. Pang, Z. Ni, J. L. Wu, Y. Zhao, *Appl. Surf. Sci.* **2018**, *434*, 273.
[15] A. Bhattacharyya, S. Chen, M. Zhu, *Exp. Polym. Lett.* **2014**, *8*, 74.
[16] W. S. Hummers, R. E. Offeman, *J. Am. Chem. Soc.* **1958**, *6*, 1339.
[17] F. Mindivan, M. Göktaş, *Polym. Bull.* **2020**, *77*, 1929.
[18] F. Mindivan, M. Göktaş, *Mater. Test.* **2019**, *61*, 1007.
[19] A. Çolak, M. Göktaş, F. Mindivan, *SN Appl. Sci.* **2020**, *2*, 375.
[20] A. Monshi, M. R. Foroughi, M. R. Monshi, *WJNSE* **2012**, *2*, 154.
[21] S. N. Danilchenko, O. G. Kukharenko, C. Moseke, I. Y. Protsenko, L. F. Sukhodub, B. Sulkio-Cleff, *Cryst. Res.Tech.* **2002**, *37*, 1234.
[22] S. S. Jikan, Z. M. Ariff, A. Ariffin, *J. Term. Anal. Calorim.* **2010**, *102*, 1011.
[23] A. S. Mohammed, A. B. Ali, M. Nesar, *J. Tribol.* **2017**, *139*, 1.
[24] H. Bahrami, A. Ramazani SA, A. Kheradmand, M. Shafiee, H. Baniasadi, *Adv. Polym. Technol.* **2015**, *34*, 1.
[25] M. Ahmad, M. U. Wahit, M. R. Abdul Kadir, K. Z. Mohd Dahlan, *Sci. World J.* **2012**, 1.
[26] W. Pang, Z. Ni, G. Chen, G. Huang, H. Huang, Y. Zhao, *RSC Adv.* **2015**, *5*, 63063.
[27] I. E. Uflyand, E. G. Drogan, V. E. Burlakova, K. A. Kydralieva, I. N. Shershneva, G. I. Dzhardimalieva, *Polym. Test.* **2019**, *74*, 178.
[28] D. L. P. Macuvele, G. Colla, K. Cesca, L. F. B. Ribeiro, C. E. da Costa, J. Nones, E. R. Breitenbach, L. M. Porto, C. Soares, M. A. Fiori, H. G. Riella, *Mater. Sci. Eng. C.* **2019**, *100*, 411.
[29] L. Meng, W. Li, R. Ma, M. Huang, J. Wang, Y. Luo, J. Wang, K. Xia, *Eur. Polym. J.* **2018**, *105*, 55.
[30] I. K. Aliyu, A. S. Mohammed, A. Al-Qutub, *Polym. Compos.* **2018**, *40*, E1301.
[31] H. Wu, L. Tong, B. Liu, C. Chen, S. Wang, J. C. Crittenden, *Appl. Surf. Sci.* **2018**, *455*, 987.
[32] G. Kandhol, H. Wadhwa, S. Chand, S. Mahendia, S. Kumar, *Vacuum* **2019**, *160*, 384.
[33] W. K. Park, J. H. Kim, *Macromol. Res.* **2005**, *13*, 206.
[34] S. G. Prolongo, A. Jimenez-Suarez, R. Moriche, A. Ureña, *Compos. Sci. Technol.* **2013**, *86*, 185.
[35] X. Gao, H. Yue, E. Guo, H. Zhang, X. Lin, L. Yao, B. Wang, *Mater. Des.* **2016**, *94*, 54.

10974628, 2021, 31, Downloaded from https://onlinelibrary.wiley.com/doi/10.1002/app.50768 by Bilecik Seyh Edebali, Wiley Online Library on [22/12/2025]. See the Terms and Conditions (https://onlinelibrary.wiley.com/terms-and-conditions) on Wiley Online Library for rules of use; OA articles are governed by the applicable Creative Commons License

[36] A. Çolak, F. Mindivan, M. Göktaş, *Nevşehir Bilim ve Teknoloji Dergisi* **2019**, *8*, 12.

SUPPORTING INFORMATION

Additional supporting information may be found online in the Supporting Information section at the end of this article.

How to cite this article: Mindivan F, Çolak A. Tribo-material based on a UHMWPE/RGOC biocomposite for using in artificial joints. *J Appl Polym Sci*. 2021;138:e50768. https://doi.org/10.1002/app.50768

10974628, 2021, 31, Downloaded from https://onlinelibrary.wiley.com/doi/10.1002/app.50768 by Bilecik Seyh Edebali, Wiley Online Library on [22/12/2025]. See the Terms and Conditions (https://onlinelibrary.wiley.com/terms-and-conditions) on Wiley Online Library for rules of use; OA articles are governed by the applicable Creative Commons License